DOI: 10.1002/asia.200600362

Glass Transitions of Ordinary and Heavy Water within Silica-Gel Nanopores

Masaharu Oguni,* Satoshi Maruyama, Kenji Wakabayashi, and Atsushi Nagoe[a]

Abstract: The dynamic properties of water confined within nanospaces are of interest given that such water plays important roles in geological and biological systems. The enthalpy-relaxation properties of ordinary and heavy water confined within silica-gel voids of 1.1, 6, 12, and 52 nm in average diameter were examined by adiabatic calorimetry. Most of the water was found to crystallize within the pores above about 2 nm in diameter but to remain in the liquid state down to 80 K within the pores less than about 1.6 nm in diameter. Only one glass transition was observed, at $T_g = 119$, 124, and 132 K for ordinary water and $T_g = 125$, 130, and 139 K for heavy water, in the 6-, 12-, and 52-nm diameter pores, respectively. On the other hand, two glass transitions were observed at $T_g =$ 115 and 160 K for ordinary water and $T_g = 118$ and 165 K for heavy water in the 1.1-nm pores. Interfacial water molecules on the pore wall, which remain in the noncrystalline state in each case, were interpreted to be responsible for the glass transitions in the region 115–139 K, and internal water molecules, surrounded only by water molecules in the liquid state, are responsible for those at 160 or 165 K in the case of the 1.1-nm pores. It is suggested that the glass transition of bulk supercooled water takes place potentially at 160 K or above due to the development of an energetically more stable hydrogen-bonding network of water molecules at low temperatures.

Keywords: calorimetry · enthalpy relaxation · glass transition · nanopores · water chemistry

Introduction

Water is abundant on the surface of the earth and plays very important roles in most natural phenomena and biological systems. Although the structure of the water molecule is simple, aggregates of these molecules show rather abnormal behavior. It is well-known that liquid water exhibits a maximum density at 277 K, and many thermodynamic properties such as heat capacity and isothermal compressibility increase as the temperature is decreased below 0 °C.[1] However, the thermodynamic and kinetic behavior of supercooled water are difficult to clarify experimentally and are still causing intense controversy. For example, the heat capacity of water droplets in an emulsified sample shows an anomaly that apparently follows a critical-point equation with the critical temperature $T_c = 228$ K on cooling.[2] On the other hand, there is the possibility that no critical phenomenon is associated with the anomaly,[3,4] and the increase in heat capacity may even originate from crystallization of emulsified water.[5] As to the kinetic properties, glass transition was reported to occur at a temperature T_g of about 136 K in vapor-deposited amorphous solid water (ASW)[6] and hyperquenched glassy water (HGW),[7] and at 129 K in low-density amorphous water (LDA).[8] Dielectric data of ASW and HGW were also analyzed to indicate a T_g of 136 K.[9] However, the possibility that $T_g = 160$–165 K was discussed based on the heat-release behavior of HGW,[10] computer simulation,[11] and the consideration[4] of thermodynamic data hitherto known, and it was indicated from thermal desorption experiments of layered nanometer-scale films of labeled ASW by McClure et al. that either a glass or a fragile-to-strong transition occurs at above 160 K.[12] Crystallization of the water below 235 K and above 150 K has so far prevented the verification of these properties in the relevant temperature range.[13]

The thermodynamic and kinetic properties of interfacial water on substrates and of a small aggregate of water droplets should also be clarified for the successful freeze-drying process of living bodies, the preparation/conservation of refrigerated foods, and the understanding of the functioning of biological systems. For example, the glass-transition temperature T_g is recognized as a boundary above and below which

[a] Prof. Dr. M. Oguni, S. Maruyama, K. Wakabayashi, A. Nagoe
Department of Chemistry
Graduate School of Science and Engineering
Tokyo Institute of Technology
2-12-1 O-okayama, Meguro-ku, Tokyo 152-8551 (Japan)
Fax: (+81) 3-5734-2222
E-mail: moguni@chem.titech.ac.jp

the biological systems function and freeze, respectively. In many systems, including polysaccharides and proteins, T_g is much higher than room temperature in the absence of water, decreases with addition of water, and becomes rather constant at around 165 K above a certain water content.[14,15] Given that such complex systems are composed of biological molecules, interfacial water of hydration interacting with the biological molecules, and water of the second hydration sphere interacting microscopically with other water molecules,[14] the mode by which the rearrangement of the biological or water molecules are connected with the glass transitions that take place at low temperatures should be clarified.

In the present study, glass-transition properties of ordinary and heavy water confined within nanometer-size pores were examined by using an adiabatic calorimeter[16] and silica gel with average pore diameters of 1.1, 6, 12, and 52 nm. We found that water aggregates, which correspond to the second hydration sphere in biological systems, undergo a glass transition at 160 and 165 K for ordinary and heavy water, respectively, and that the interfacial water on the pore wall exhibits a glass transition over the range 115–139 K and is composed roughly of one layer.

Calorimetric Determination of the Presence of a Glass Transition

The presence of a calorimetric glass transition is usually identified by differential scanning calorimetry (DSC) through a jump in heat capacity. However, it can be rather difficult to identify if the jump in heat capacity is small or the mode of molecular rearrangement that causes the glass transition has some component in the relaxation times. Adiabatic calorimetry is a powerful tool for the identification of glass transitions even in such situations as it functions like very low frequency spectroscopy; the timescale of the relaxation to be detected ranges from 10^6 to 10^2 s.[17,18] This is very important, as the longer the characteristic timescale, the more clearly separated the different modes of motion are in the temperature ranges over which the characteristic enthalpy-relaxation properties appear. The relaxation accompanying a glass transition proceeds from non-equilibrium to equilibrium states. As the non-equilibrium state at a certain constant temperature varies depending on how the sample was brought to that temperature, the rate of enthalpy relaxation is altered by the thermal history, such as the rate of precooling. Figure 1 illustrates the general behavior, over the glass-transition temperature range, of the relaxation time τ of molecular rearrangement, the enthalpy H, and the enthalpy relaxation rate $-dH/dt$ of the process with a single characteristic time. That is, there is no complex behavior originating from a distribution of relaxation times. The equilibrium relaxation time τ increased with decreasing temperature. When the liquid vitrified through rapid cooling, τ deviated from the equilibrium dependence at relatively high temperature (Figure 1a),[19] and H became much higher than for the equilibrium situation (Figure 1b). When the temperature of the glass was increased for measurements, τ became short and gradually approached a calorimetric timescale between 10^6 and 10^2 s. Then, an exothermic enthalpy-relaxation effect was first observed as H started to relax, that is, decrease, towards its equilibrium value; $-dH/dt$ increased with an increase in temperature due to the shortening of τ. Further increase in the temperature resulted in H crossing the equilibrium line at around T_g and taking on smaller values than at equilibrium; $-dH/dt$ exhibited a positive peak, became zero at the crossing of H with the

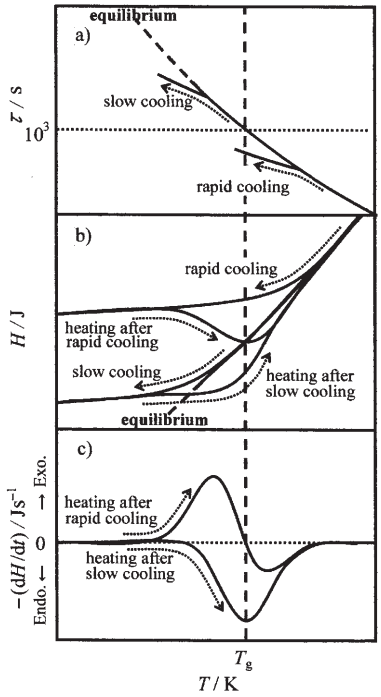

Figure 1. Relationship between a) the relaxation time τ, b) the enthalpy H, and c) the spontaneous enthalpy-relaxation rate $-dH/dt$ and temperature, observed calorimetrically in a glass transition with a single characteristic time for the molecular rearrangement. The glass-transition temperature was determined empirically as the point at which the rapidly cooled sample showed a change (against temperature) in $-dH/dt$ from positive to negative and the slowly cooled sample showed a minimum $-dH/dt$ value.[16,17]

Abstract in Japanese:

ナノ空間に閉じ込めた水は自然の多くの局面で重要な役割を果たしており，その動的性質は興味深い。平均幅 1.1 nm のスリット，および平均直径 6, 12, 52 nm のシリカゲル細孔中にある軽水および重水のエンタルピー緩和性質を断熱法熱測定により追跡した。低温で細孔内部の水は，およそ 2 nm 以上の細孔中では結晶化して氷になり，およそ 1.6 nm 以下では液体のままであった。水分子1層程度から成る界面水は，常に液体状態にあり，1.1, 6, 12, 52 nm におけるガラス転移温度は軽水でそれぞれ 115, 119, 124, 132 K，重水でそれぞれ 118, 125, 130, 139 K であった。1.1 nm の内部水は，水分子のみにより囲まれて水素結合した水分子に相当し，軽水，重水においてそれぞれ 160, 165 K でガラス転移を示した。水のガラス転移温度は水分子の水素結合ネットワークが発達するとともに高くなり，バルク過冷却水では 160 K あるいはそれ以上にあることを，この結果は示唆している。

equilibrium line, and then took on negative values (Figure 1c). As the temperature was increased further, τ became shorter than 10^2 s, and the liquid exhibited no relaxation phenomenon in the calorimetric timescale; $-dH/dt$ returned to zero while the glass reached its equilibrium state within a duration of the order of 10^2 s. On the other hand, when the liquid vitrified through slow cooling, τ and H deviated from their respective equilibrium lines at relatively lower temperatures, and H was considerably lower than that of the rapidly cooled liquid. Upon heating the liquid for measurements, an endothermic enthalpy relaxation appeared after H crossed the equilibrium line and took on lower values than at equilibrium; $-dH/dt$ exhibited a negative peak. As τ became shorter with increasing temperature, H, which had deviated below the equilibrium line, gradually returned to it at essentially the same temperature as in the case for the rapidly cooled liquid.

Consequently, the observation of a set of exothermic and endothermic $-dH/dt$ values for the rapidly and slowlycooled samples, respectively (Figure 1c), indicates the presence of a glass transition.[17,18] The T_g value at which τ became 10^3 s was determined empirically as the temperature at which the rapidly cooled sample showed a change (against temperature) in $-dH/dt$ from heat-evolution to heat-absorption effects, and the slowly cooled sample showed a maximum in the heat-absorption effect.[16,17]

Results and Discussion

The silica-gel materials CARiACT Q-50, Q-10, Q-6, and Q-3 were utilized. The pores into which water molecules were introduced were formed as gaps between the aggregates of silica. The average pore diameter for Q-50 silica gel was estimated by mercury porosimetry to be 52 nm according to the data of Fuji Silysia Chemical Ltd. Japan. The pore sizes for Q-10, Q-6, and Q-3 were estimated from data for nitrogen-gas absorption/desorption against its vapor pressure at 77 K. Figure 2a and c shows the isotherms for Q-6 and Q-10, respectively. The curves are of the type that is well-analyzed by the Barret–Joyner–Halenda (BJH) method.[20] The results of the pore-size distribution are shown in Figure 2b and d. The pores have an average diameter of 6 and 12 nm, respectively, and a distribution of diameters that range roughly from 2 to 16 nm and from 2 to 20 nm, respectively. This indicates that the silica gels are mixed pore solids of different pore diameters. Figure 3a shows the data for nitrogen-gas absorption/desorption for Q-3. The curves are of the type that is well-analyzed by the micropore (MP) method.[21] The data were analyzed by assuming slit-type micropores, and the distribution of pore diameters is shown in Figure 3b. The pores have an average diameter of 1.1 nm with a distribution of diameters ranging from 0.4 to 2 nm.

Calorimetry was performed in the heating direction with repetition of energy supply and thermometry periods under adiabatic conditions. Most of the water crystallized as ice on cooling before measurement in the cases of the pores with

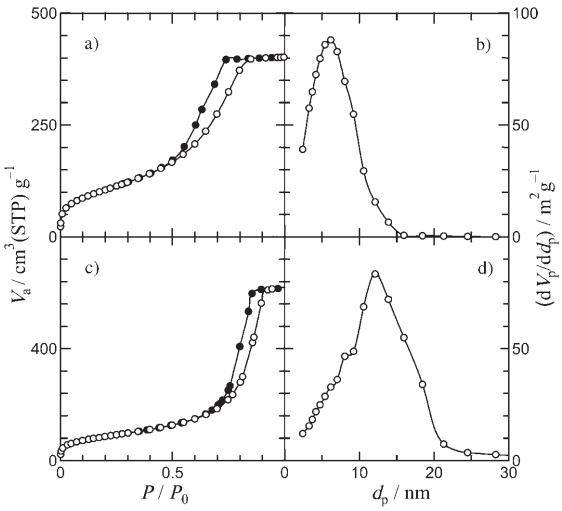

Figure 2. a) and c) Nitrogen-gas absorption and desorption isotherms as a function of the vapor pressure at 77 K. b) and d) Distribution of pore diameters as analyzed by the BJH method[20] for silica gels Q-6 and Q-10, respectively. ○ = absorbed gas measured with increasing vapor pressure, ● = absorbed gas measured with decreasing pressure. The volume of nitrogen gas absorbed is that under standard conditions (STP) of 0 °C and one atmosphere pressure. The pores were assumed in the analysis to be cylindrical.

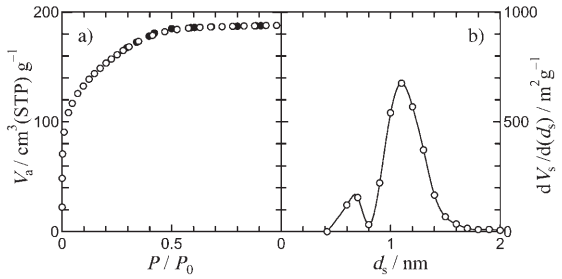

Figure 3. a) Nitrogen-gas absorption and desorption isotherms as a function of the vapor pressure at 77 K. b) Distribution of pore thickness as analyzed by the MP method[21] for silica gel Q-3. ○ = absorbed gas measured with increasing vapor pressure, ● = absorbed gas measured with decreasing pressure. The volume of nitrogen gas is that under standard conditions (STP) of 0 °C and one atmosphere pressure. The pores were assumed in the analysis to be slitlike.

6, 12, and 52 nm average diameters. In the 1.1-nm pores, as there was a certain pore-size distribution present as shown in Figure 3b, only a small part of the water crystallized; the majority remained in the liquid state down to 80 K. Figure 4a–d shows the heat capacities experimentally derived from a mixture of ordinary water and ice confined within 1.1-, 6-, 12-, and 52-nm pores, respectively. The big heat-capacity peaks found at 260–270 K in Figure 4b–d are due to fusion of ice.[23] In the 1.1-nm pores, a small hump was found at 227 K and a peak at around 240 K. Given that the data around 227 K connected smoothly with those of the sample that was cooled only to 235 K and expected to remain entirely in the liquid state, the hump at 227 K may reflect the order/disorder process of water molecules in the

CHEMISTRY
AN ASIAN JOURNAL

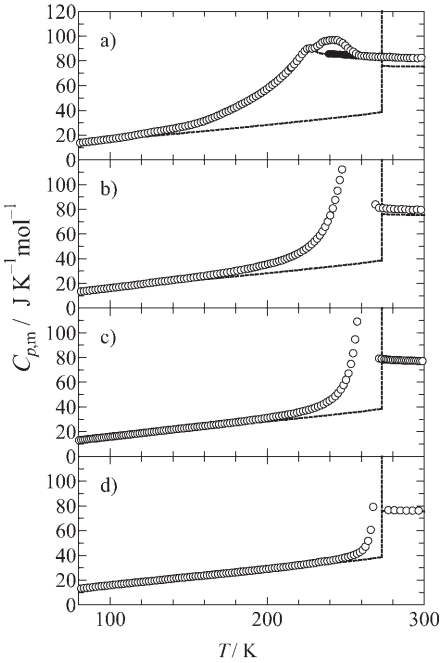

Figure 4. Heat capacities of mixtures of ordinary water and ice (H_2O) confined within the voids of silica gel of a) 1.1-nm, b) 6-nm, c) 12-nm, and d) 52-nm average pore diameter. Dotted lines represent the literature results of bulk water and ice (H_2O),[22] and filled circles in a) represent the data obtained for the sample cooled to 235 K and measured in the heating direction.

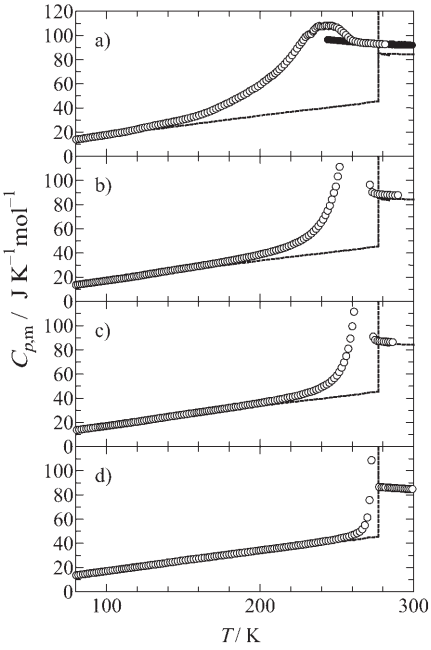

Figure 5. Heat capacities of mixtures of heavy water and ice (D_2O) confined within the voids of silica gel of a) 1.1-nm, b) 6-nm, c) 12-nm, and d) 52-nm average pore diameter. Dotted lines represent the literature results of bulk water and ice (D_2O),[24] and filled circles in a) represent the data obtained for the sample cooled to 240 K and measured in the heating direction.

liquid state,[2] and the peak at around 240 K is attributed to fusion of ice formed in part of the water.[23] Figure 5 a–d shows the heat capacities derived from a mixture of heavy water and ice confined within 1.1-, 6-, 12-, and 52-nm pores, respectively. This behavior resembles that of ordinary water except that the temperatures of fusion are a little higher than those in Figure 4 in the respective pores.

Figure 6 a–d shows the rate of spontaneous heat release or absorption, observed in the thermometry periods of heat-capacity measurements upon intermittent heating, of ordinary water confined within the 1.1-, 6-, 12-, and 52-nm pores, respectively. In the latter three cases, heat-release and -absorption effects appeared in the range 100–140 K. When the sample was cooled rapidly in this temperature range before measurement, heat-release (positive $-dH_m/dt$) and then heat-absorption (negative $-dH_m/dt$) effects were observed in the measurements. When the sample was cooled slowly, on the other hand, only the heat-absorption effect was observed. This dependence reflects the enthalpy relaxation of the water due to its structural change and is characteristic of a glass transition as described above. The T_g value, at which τ becomes 1 ks, was estimated to be 119, 124, and 132 K for the 6-, 12-, and 52-nm pores, respectively, according to the empirical relation stated above.[16,17] In the case of the 1.1-nm pores, two sets of heat release and absorption effects were found in the ranges 90–130 and 130–170 K, indicating the presence of two glass transitions. The T_g values were estimated in the same way to be 115 and 160 K. Figure 7 a–d shows the rate of similar spontaneous heat release or absorption observed for heavy water confined within the 1.1-, 6-, 12-, and 52-nm pores, respectively. The temperature and cooling-rate dependence is quite similar to that for ordinary

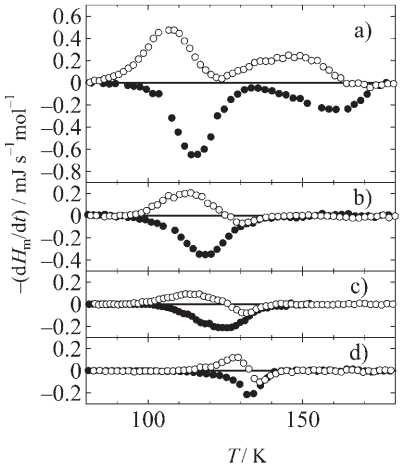

Figure 6. Temperature dependence of the rates of spontaneous heat release and absorption, observed in the heat-capacity measurements of ordinary water (H_2O) by an intermittent heating method. Average pore diameter: a) 1.1 nm, b) 6 nm, c) 12 nm, d) 52 nm. ○ = sample cooled rapidly at around 5 K min^{-1} before the measurements, ● = sample cooled slowly at 10 mK min^{-1}. The systematic heat-evolution and -absorption effects for the rapidly and slowly cooled samples are characteristic of a glass transition, and there are two transitions found in the case of the 1.1-nm pores.

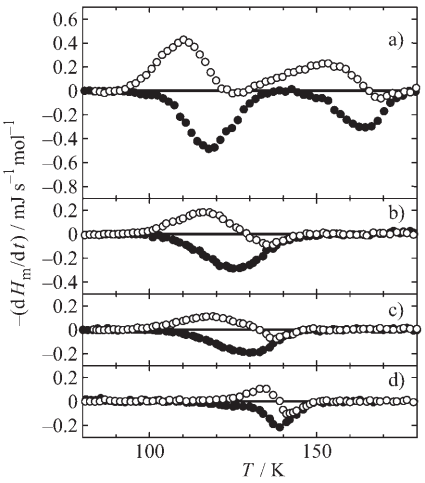

Figure 7. Temperature dependence of the rates of spontaneous heat release and absorption, observed in the heat-capacity measurements of heavy water (D_2O) by an intermittent heating method. Average pore diameter: a) 1.1 nm, b) 6 nm, c) 12 nm, d) 52 nm. ○ = sample cooled rapidly at around 5 K min^{-1} before the measurements, ● = sample cooled slowly at 10 mK min^{-1}. The characteristic behavior of a glass transition is present as in the case of H_2O (Figure 6).

water. The T_g value was estimated to be 125, 130, and 139 K for the 6-, 12-, and 52-nm pores, respectively. In the case of the 1.1-nm pores, the two T_g values were estimated to be 118 and 165 K.

The water confined within the pores is potentially divided into two parts: interfacial water and internal water.[25] The molecules of the former interact with silanol groups to form hydrogen bonds, and the latter, located in the central part of the pore, interact only with other water molecules. As the silanol groups are arrayed in a rather random fashion, the interfacial water constructs no neat hydrogen-bonding network like in ice and undergoes no crystallization as ice. Therefore, in the cases of the 6-, 12-, and 52-nm pores, it is expected that the interfacial water molecules are arranged in a rather disordered manner and exhibit a glass transition, whereas all the internal water crystallize as ice. In the case of the 1.1-nm pores, the majority of the internal water is interpreted as being in the liquid state even at low temperatures[26] and shows a glass transition in a temperature region different from that of the interfacial water. It is reasonable to understand the glass transition at low temperature as originating from the freezing of the configuration of the interfacial water, in that T_g decreases quite systematically as the pore size decreases (132, 124, 119, and 115 K for ordinary water and 139, 130, 125, and 118 K for heavy water in the cases of the 52-, 12-, 6-, and 1.1-nm pores, respectively), and that the heat-release/absorption effects increase systematically with decreasing pore size with a corresponding increase in the fraction of interfacial water. The decrease of T_g with decreasing pore size is understood as indicating that the formation of a strong hydrogen-bonding network is interrupted gradually as the number of water molecules within the pores is decreased. The interfacial as well as internal water molecules tend to form the hydrogen-bonding network at low temperatures. However, the interfacial water molecules form hydrogen bonds with the silanol groups, which are located rather randomly and are fixed in position, so an energetically ideal arrangement of water molecules for network formation cannot be attained. In such a situation, the interfacial water molecules are considered to form energetically less optimized hydrogen bonds, resulting in bonds that are rather easy to break for rearrangements.

On the basis of the above assignment of the T_g value of the interfacial water, the glass transitions at $T_g = 160$ K for ordinary water and $T_g = 165$ K for heavy water in the 1.1-nm pores originate from the freezing of the configuration of the internal water, namely, water molecules interacting only with other water molecules. The result that the T_g value of the internal water is higher than that of the interfacial water is understood as follows. The water molecule in the interface forms hydrogen bond(s) with silanol group(s). Then, as the silanol groups are fixed in their positions as described above, the rearrangement of the water molecule requires the breaking of the bond(s) by movement of the water molecule itself, and the presence of the silanol groups interrupts the free movement of the water molecule. Such situations cause the activation energy for the rearrangement of the interfacial water molecule to increase. The situation of the interfacial water molecule is rather similar at low and room temperature, because the hydrogen-bonding network cannot be developed due to the randomness in and the immobility of the positions of the silanol groups. This results in a mostly temperature-independent activation energy $\Delta\varepsilon_a$ and, therefore, the Arrhenius behavior of the relaxation times. On the other hand, in the internal water at room temperature, the formation of the hydrogen bonds of the water molecules is not necessarily complete, and the breaking of the hydrogen bond(s) proceeds in concert with the movement of the surrounding water molecules, resulting in a relatively small activation energy and thus short relaxation time, as seen in bulk water.[27] At low temperatures, however, the water molecules develop a hydrogen-bonding network with stronger bonds so as to decrease the energy of the system. This causes the $\Delta\varepsilon_a$ for the rearrangement of the molecules at low temperatures to increase, as rearrangement requires the breaking of more and stronger hydrogen bonds here than at room temperature. The $\Delta\varepsilon_a$ of the internal water is interpreted to be larger than that of the interfacial water at the low temperatures at which the glass transitions take place. The values of $T_g = 160$ or 165 K for the internal ordinary and heavy water, respectively, are potentially related to the intrinsic property of bulk water, given that the water molecules are surrounded only by other water molecules in both cases and that the T_g value is consistent with the prediction by Angell et al.[10] and McClure et al.,[12] and the observation[28] that, when kept for 60 s at 148 K, HGW and LDA did not transform into each other.

One might consider that the heat-release and -absorption effects at around 160–165 K are due to crystallization of

CHEMISTRY
AN ASIAN JOURNAL

water and fusion of the minute ice particles formed.[23] The phenomena of heat release and subsequent absorption upon heating appearing for the rapidly cooled liquid, but only heat absorption for the sufficiently annealed one, were observed in some cases of crystallization/fusion processes. However, in the case of the rapidly cooled liquid, the subsequent heat-absorption effect should be equal to or larger than the heat-release effect. In reality, the absorption effect observed was much smaller than the release effect in the rapidly cooled sample. This indicates that the anomaly at around 160 K is not attributed to the crystallization as and fusion of ice.

On the basis of the above interpretation, the fraction of ice formed in the central portion of the pore was determined from the enthalpy of fusion. The fractions of ice determined were 0.69, 0.85, and 0.96 for ordinary water and 0.74, 0.85, and 0.97 for heavy water in the 6-, 12-, and 52-nm pores, respectively. In the case of the 1.1-nm pores, provided that the heat-capacity peak at around 240 K was caused by fusion, the fraction of ice formed was estimated to be 0.059 and 0.090 of all the ordinary and heavy water, respectively. With the assumption that the 6-, 12-, and 52-nm pores were cylindrical and that the interfacial water and ice have the same density, the thickness of the interfacial water layer was estimated from those fractions to be about 0.4 nm. This value is in agreement with those in the literature determined by different methods.[25] Given that the van der Waals diameter of a water molecule is about 0.4 nm, the thickness of the layer of interfacial water corresponds roughly to one layer of molecules. As only three water molecules can be arrayed within the 1.1-nm-or-so slit pore, the present result indicates that, so long as a water molecule is surrounded only by other water molecules (including interfacial water molecules) in an energetically appropriate way, the relaxation time of the water molecule would give a T_g of about 160 K. Furthermore, by taking into account the real distribution of pore sizes present and the fact that 0.06–0.09 of the water molecules crystallized as ice in the Q-3 silica gel, the water molecules introduced into the pores remain in the noncrystalline state to 80 K only for pores less than around 1.6 nm in diameter and crystallize for pores above 2 nm in diameter.

Faraone et al.[29] reported the temperature dependence of the relaxation times for water confined in silica matrices MCM-41-S with 1.4- and 1.8-nm pore diameters. They determined the relaxation times by using a quasielastic neutron-scattering technique and analyzing the data with a relaxing cage model, and claimed a bend in the relaxation times at around 225 K with non-Arrhenius and Arrhenius behavior above and below that temperature, respectively. The extrapolation of the relaxation times below 225 K indicates that a glass transition with $\tau = 10^3$ s occurs at around 80 K. As they did not distinguish between internal and interfacial water, the discrepancy between the present T_g result and their temperature dependence of the relaxation times remains an open question to be solved.

Conclusions

The thermal properties and glass-transition behavior of water confined within silica-gel pores ranging from 1.1 to 52 nm in average diameter were disclosed by adiabatic calorimetry. Water located in the central part of the pores remains in the noncrystalline state down to 80 K in the pores below roughly 1.6 nm in diameter, and crystallizes within those larger than 2 nm in diameter. The dynamic properties of water within the pores are quite different for water molecules interacting with silanol groups and those surrounded only by other water molecules. The glass transition of the former takes place at 115–139 K depending on the pore size, and that of the latter at 160 and 165 K for ordinary and heavy water, respectively. The situation would be same even if the silanol groups were replaced with other hydrophilic groups such as those in proteins and polysaccharides, as found in a hydrated protein system.[30] Notably, in this respect, the interfacial water is mobile down to 120 K or so. Also, the T_g of 160 K for the internal water is very close to that of 160–165 K predicted for bulk supercooled water by some research groups[4,10,11] and the T_g of 165 K in aqueous solutions of proteins and polysaccharides.[14,15]

Experimental Section

Preparation and Porosimetry

Silica-gel materials CARiACT Q-50, Q-10, Q-6, and Q-3 were provided by Fuji Silysia Chemical Ltd., Japan. They were particles with apparent diameters of 2–3 mm. The pore sizes for Q-10, Q-6, and Q-3 were estimated by using a Mini-type Japan Bell porosimeter. The silica gels were cleaned with distilled water, dried at 200 °C in vacuum, and loaded at room temperature with distilled water under completely degassed conditions.

Calorimetry

Heat-capacity measurements were carried out under adiabatic conditions with the calorimeter already reported.[16] The silica-gel sample loaded with water above was introduced into a calorimeter cell (20 cm^3), and the cell was sealed with indium wire under an atmosphere of helium gas. After the calorimetric system was set up at room temperature to achieve adiabatic conditions, the cell was cooled to the temperature at which the measurement was started. To observe the presence of a glass transition, the cooling rate was adjusted to 5 $K\,min^{-1}$ for one set of measurements and 10 $mK\,min^{-1}$ for the other. The heat capacities were measured by an intermittent heating method; energy supply and thermometry were repeated under adiabatic conditions. When heat release or absorption occurred due to glass or phase transition of the water within the pores, they were detected as a spontaneous temperature rise or fall, respectively, and the rate of enthalpy relaxation $-dH/dt$ was evaluated as Equation (1):

$$-dH/dt = C\,(dT/dt)/n_w \quad (1)$$

in which C is the gross heat capacity of the cell and n_w is the amount of water within the pores. The average heating rate for the measurements was about 0.1 $K\,min^{-1}$, which is between the above rapid (5 $K\,min^{-1}$) and slow (10 $mK\,min^{-1}$) cooling rates. The heat capacities of the water within the pores were derived by subtracting the contributions of the empty cell and the silica gel dried at 200 °C from the experimental results of water-loaded silica gel. The inaccuracy and imprecision of the heat-capacity values derived were estimated previously to be less than 0.3 % and 0.06 %, respectively.[16]

Acknowledgements

We thank Fuji Silysia Chemical Ltd., Japan for providing us with the silica gel utilized in the present work. This work was financially supported partly by a Grant-in-Aid for Scientific Research (Grant 18350003) from theMinistry of Education, Culture, Sports, Science, and Technology, Japan.

[1] F. Franks, *A Comprehensive Treatise*, Plenum Press, New York, **1972**.
[2] C. A. Angell, W. J. Sichina, M. Oguni, *J. Phys. Chem.* **1982**, *86*, 998–1002.
[3] a) P. H. Poole, F. Sciortino, U. Essmann, H. E. Stanley, *Nature* **1992**, *360*, 324–328; b) S. Sastry, P. G. Debenedetti, F. Sciortino, H. E. Stanley, *Phys. Rev. E* **1996**, *53*, 6144–6154; c) F. Sciortino, P. H. Poole, U. Essmann, H. E. Stanley, *Phys. Rev. E* **1997**, *55*, 727–737.
[4] a) F. W. Starr, C. A. Angell, H. E. Stanley, *Phys. A* **2003**, *323*, 51–66; b) F. W. Starr, C. A. Angell, E. L. Nave, S. Sastry, A. Acala, F. Sciortino, H. E. Stanley, *Biophys. Chem.* **2003**, *105*, 573–583.
[5] G. P. Johari, *J. Chem. Phys.* **1997**, *107*, 10154–10165.
[6] a) M. Sugisaki, H. Suga, S. Seki, *Bull. Chem. Soc. Jpn.* **1968**, *41*, 2591–2599; b) A. Hallbrucker, E. Mayer, G. P. Johari, *J. Chem. Phys.* **1989**, *93*, 4986–4990.
[7] a) G. P. Johari, A. Hallbrucker, E. Mayer, *Nature* **1987**, *330*, 552–553; b) A. Hallbrucker, E. Mayer, G. P. Johari, *Philos. Mag. B* **1989**, *60*, 179–187; c) I. Kohl, L. Backmann, A. Hallbrucker, E. Mayer, T. Loerting, *Phys. Chem. Chem. Phys.* **2005**, *7*, 3210–3220.
[8] A. Hallbrucker, E. Mayer, G. P. Johari, *J. Phys. Chem.* **1989**, *93*, 7751–7752.
[9] G. P. Johari, *J. Chem. Phys.* **2005**, *122*, 144508/1–144508/10.
[10] a) V. Velikov, S. Borick, C. A. Angell, *Science* **2001**, *294*, 2335–2338; b) Y. Yu, C. A. Angell, *Nature* **2004**, ***427***, 717–720.
[11] N. Giovambattista, C. A. Angell, F. Sciortino, H. E. Stanley, *Phys. Rev. Lett.* **2004**, *93*, 047801/1–047801/4.
[12] S. M. McClure, D. J. Safarik, T. M. Truskett, C. B. Mullins, *J. Phys. Chem. B* **2006**, *110*, 11033–11036.
[13] O. Mishima, H. E. Stanley, *Nature* **1998**, *396*, 329–335.
[14] G. Sartor, G. P. Johari, *Biophys. J.* **1994**, *66*, 249–258.
[15] J. L. Green, J. Fan, C. A. Angell, *J. Phys. Chem.* **1994**, *98*, 13780–13790.
[16] H. Fujimori, M. Oguni, *J. Phys. Chem. Solids* **1993**, *54*, 271–280.
[17] M. Oguni, T. Matsuo, H. Suga, S. Seki, *Bull. Chem. Soc. Jpn.* **1975**, *48*, 379–391.
[18] H. Suga, S. Seki, *Faraday Discuss. Chem. Soc.* **1980**, *69*, 221–240.
[19] a) H. Fujimori, M. Oguni, *Solid State Commun.* **1995**, *94*, 157–162; b) M. Oguni, *J. Non-Cryst. Solids* **1997**, *210*, 171–177.
[20] E. P. Barrett, L. G. Joyner, P. P. Halenda, *J. Am. Chem. Soc.* **1951**, *73*, 373–380.
[21] R. Sh. Mikhail, S. Brunauer, E. E. Bodor, *J. Colloid Interface Sci.* **1968**, *26*, 45–53.
[22] O. Haida, T. Matsuo, H. Suga, S. Seki, *J. Chem. Thermodyn.* **1974**, *6*, 815–825.
[23] a) R. Schmidt, E. W. Hansen, M. Stoecker, D. Akporiaye, O. H. Ellestad, *J. Am. Chem. Soc.* **1995**, *117*, 4049–4056; b) A. Schreiber, I. Ketelsen, G. H. Findenegg, *Phys. Chem. Chem. Phys.* **2001**, *3*, 1185–1195; c) K. Morishige, H. Iwasaki, *Langmuir* **2003**, *19*, 2808–2811.
[24] O. Haida, H. Suga, S. Seki, *J. Glaciol.* **1979**, *22*, 155–16464.
[25] K. Morishige, K. Kawano, *J. Chem. Phys.* **1999**, *110*, 4867–4872.
[26] T. Takamuku, M. Yamagami, H. Wakita, Y. Masuda, T. Yamaguchi, *J. Phys. Chem. B* **1997**, *101*, 5730–5739.
[27] S. Kittaka, S. Takahara, T. Yamaguchi, M.-C. B. Funel, *Langmuir* **2005**, *21*, 1389–1397.
[28] G. P. Johari, A. Hallbrucker, E. Mayer, *Science* **1996**, *273*, 90–92.
[29] A. Faraone, L. Liu, C.-Y. Mou, C.-W. Yen, S.-H. Chen, *J. Chem. Phys.* **2004**, *121*, 10843–10846.
[30] K. Kawai, T. Suzuki, M. Oguni, *Biophys. J.* **2006**, *90*, 3732–3738.

Received: October 26, 2006
Revised: January 11, 2007

